Comparison of Gold Bonding with Mercury Bonding

Kraka, Elfi; Filatov, Michael; Cremer, Dieter

Published in:
Croatica Chemica Acta

Publication date:
2009

CROATICA CHEMICA ACTA
CCACAA, ISSN-0011-1643, ISSN-1334-417X
Croat. Chem. Acta **82** (1) (2009) 233-243.
CCA-3312

Original Scientific Paper

Comparison of Gold Bonding with Mercury Bonding*

Elfi Kraka,[a] Michael Filatov,[b] and Dieter Cremer[a,]**

[a]*Department of Chemistry, University of the Pacific, 3601 Pacific Avenue, Stockton, CA 95211, USA*
[b]*Department of Chemistry, Zernike Institute for Advanced Materials, University of Groningen, Nijenborgh 4, 9747AG Groningen, Netherlands*

RECEIVED MAY 2, 2008; REVISED AUGUST 8, 2008; ACCEPTED SEPTEMBER 9, 2008

Abstract. Nine AuX molecules (X = H, O, S, Se, Te, F, Cl, Br, I), their isoelectronic HgX^+ analogues, and the corresponding neutral HgX diatomics have been investigated using NESC (Normalized Elimination of the Small Component) and B3LYP theory to determine relativistic effects for bond dissociation energies (BDEs), bond lengths, dipole moments, and charge distributions. Relativistic effects are substantially larger for AuX than HgX molecules. AuX bonding has been contrasted with HgX bonding considering the effects of relativity, charge transfer and ionic bonding, 3-electron *versus* 2-electron bonding, residual π-bonding, lone pair repulsion, and the d-block effect. The interplay of the various electronic effects leads to strongly differing trends in calculated BDEs, which can be rationalized with a simple MO model based on electronegativity differences, atomic orbital energies, and their change due to scalar relativity. A relativistic increase or decrease in the BDE is directly related to relativistic changes in the 6s orbital energy and electron density.

Keywords: NESC/B3LYP, bonding theory, relativistic effects, gold halides, gold chalcogenides

INTRODUCTION

Chemical bonding of gold and mercury to main group elements is strongly influenced by scalar relativistic effects,[1] which has been amply discussed in several review articles[2–7] and a large number of primary research articles on AuX[8–34] and HgX molecules.[35–60] It is well known that the mass increase of electrons moving close to a heavy nucleus leads to a lowering of the corresponding orbital energies accompanied by orbital contraction and an overall stabilization of the atom as reflected by a more negative energy. In the case of gold and mercury, these relativistic effects involve especially the 6s electrons. Relativity increases the ionization potentials (IPs) of the 6s electrons, increases the electronegativity of Au and Hg, and reduces atomic radius and volume of the two metal (M) atoms. One might argue that orbital contraction is responsible for the fact that in most cases relativistic MX bond lengths are shorter than their non-relativistic counterparts. However, orbital contraction and bond length reduction are just parallel, but result from different physical effects as was first shown by Ziegler, Snijders, and Baerends.[9] Orbital contraction is a result of mixing in of higher bound and continuum orbitals due to the action of the scalar relativistic operator, which leads to cutting of the tails of the valence orbitals[9] whereas bond length contraction is caused by increased orbital overlap among core orbitals for decreasing *R* and a subsequent larger scalar relativistic energy lowering.

Relativistic bond length reduction does not necessarily imply that bonds become stronger, as one would expect in the case of bonding between atoms of the first rows of the periodic table. For example, orbital contraction may lead to a reduction of charge transfer from M to its partner atom X thus decreasing the polar (ionic) character of the bond, which normally causes bond weakening. On the other hand, lowering the energy of the 6s orbital and reducing the covalent radius will lead to a new bonding situation characterized by different orbital interactions (depending on overlap and orbital energy).

For the purpose of assessing and predicting changes in the bond properties of AuX and HgX molecules as caused by relativistic effects, we will use relativistic and non-relativistic quantum chemical methods and calculate for X = H; F, Cl, Br, I (halogens); O, S, Se, Te (chalcogens) bond length, bond dissociation energy (BDE), charge distribution, and dipole moment.

* Dedicated to Professor Zvonimir Maksić on the occasion of his 70th birthday.
** Author to whom correspondence should be addressed. (E-mail: dcremer@pacific.edu)

Including into the analysis also the corresponding HgX^+ ions, which are isoelectronic with their AuX counterparts, will facilitate comparison between AuX and HgX. In total, 27 MX diatomics are investigated with the objective of answering the following questions:

1) How do the BDEs of AuX molecules compare with those of their HgX and HgX^+ analogues?

2) Does relativity increase or decrease the BDE values in these cases?

3) Are the changes in BDE values caused by scalar relativistic effects parallel to the corresponding changes in the bond length?

4) How can one rationalize trends in relativistic and non-relativistic bond properties with the help of a suitable model?

5) Finally, we will also consider the question whether the methods used in this work lead to a reliable description of the properties of AuX and HgX molecules.

This work is structured in the following way. In the following section, we will describe the computational methods applied in this investigation. Results of the relativistic calculations will be presented and contrasted with those of non-relativistic calculations. A bonding model will be developed, which will be used to explain general trends in relativistic corrections and changes in AuX and HgX bonding in dependence of the electronic nature of element X. And finally, the conclusions of this work will be presented.

COMPUTATIONAL METHODS

In previous work, we have systematically extended the regular approximation of Baerends and co-workers[60,61] in a way that it can routinely be applied with any wave function or density functional method.[62–64] Especially, we have shown[65,66] that the regular approximation is naturally connected to the normalized elimination of the small component (NESC) of Dyall.[67,68] In recent work,[69,70] we have systematically compared NESC/CCSD(T) (coupled cluster (CC) theory including all single (S) and double (D) excitations combined with a perturbative treatment of the triple excitations (T))[71] and NESC/DFT (density functional theory).[72] A major result of this investigation was that NESC/DFT results obtained with the B3LYP hybrid functional[73–75] are in reasonable agreement with the results of the more accurate NESC/CCSD(T) method. In general, NESC is superior to the most popular variants of the regular approximation,[60,61] which in turn are more reliable than the corresponding Douglas-Kroll approximations. Hence, we will use in this work exclusively NESC/B3LYP for the relativistic and B3LYP for the non-relativistic reference calculations.

For Au and Hg, we used (22s19p12d9f) primitive basis sets of Dyall[76a] that were converted *via* the contraction scheme (222231211111111/5311111111111/-42111111/42111) to [15s13p8d5f] contracted basis sets. The contraction was chosen to minimize basis set superposition errors (BSSE), which were determined by the counterpoise method.[77] In all cases tested, the BSSE was smaller than 0.5 kcal mol^{-1} and therefore was no longer considered. The Au and Hg basis sets are of VDZ quality in the core space, however of VTZ quality in the valences space. Accordingly, they were combined with Dunning aug-cc-pVTZ basis sets for elements of the first four periods.[78] For elements of the 5th period (Te, I), Dyall basis sets of the type (22s16p12d2f)[12s11p7d2f] were used.[76b] The basis sets chosen were tested and confirmed as being reasonable by calculating ionization potentials (IPs) for the atoms and comparing them with experimental values.[79]

In this work, only scalar relativistic corrections were considered. Spin-orbit coupling (SOC) effects can become large in magnitude for $Z > 50$ and when the fractional occupation of p- and d-orbitals is significant. In the case of HgO, the energy lowering due to SOC was calculated to be 2–3 kcal mol^{-1} depending on method and basis set,[36] which may be considered as an upper limit for the mercury molecules investigated. In the case of $AuO(^2\Pi)$, a SOC splitting of 4 kcal mol^{-1} between the 1/2 and 3/2 levels was found.[18] Hence, the SOC effect will change the calculated BDE by some kcal mol^{-1} (where changes in bond lengths have also to be considered) and may slightly affect also trends in BDE values. In view of the fact that we are primarily interested in the overall bonding behavior in AuX and HgX molecules, we consider SOC as a second order effect and discard it in this work. Also, we do not calculate vibrational and thermal corrections to the BDE because these are smaller for the heavy diatomics than the SOC effects.

In the case of the HgX^+ diatomics, dissociation according to reaction (1) rather than reaction (2)

$$HgX^+ \rightarrow Hg^+\left(^2S\right) + X \quad (1)$$

$$HgX^+ \rightarrow Hg\left(^1S\right) + X^+ \quad (2)$$

turned out to be the preferred in all cases and therefore (1) is exclusively discussed in this work although dissociation according to (2) was also calculated.

Relativistic corrections to the BDE, charge transfer, and dipole moment values were calculated utilizing NESC/B3LYP and B3LYP bond lengths. For the analysis of the charge transfer from or to M, the natural bond order (NBO) analysis was applied at the NESC/B3LYP and B3LYP levels of theory.[80] Since NBO charges are not always conclusive, especially if M and X possess

Table 1. Properties of AuX and HgX as calculated with NESC/B3LYP or B3LYP[(a)]

Molecule (State)	R(MX)Relat. Å	R(MX)Non-relat. Å	ΔR(MX) Å	BDE Relat. kcal mol^{-1}	ΔE Relat. kcal mol^{-1}	q(M) Relat. *e*	q(M)Non-Relat. *e*	Δq(M)(Relat. – Non-Relat.) *e*	dipole Relat. debye	dipole Non-relat. debye	Δdipole debye
AuH ($^1\Sigma^+$)	1.535 (1.528)	1.746	0.210	74.2 (74.3)	22.7	0.072	0.445	−0.373	1.40	3.37	−1.97
AuO ($^2\Pi$)	1.882 (1.912)	2.163	0.281	52.8 (53.7)	7.2	0.538	0.759	−0.221	3.39	5.53	−2.14
AuS ($^2\Pi$)	2.207	2.464	0.257	59.5 (59.7)	10.8	0.325	0.642	−0.317	2.63	5.15	−2.52
AuSe ($^2\Pi$)	2.341	2.573	0.232	53.5 (57.2)	6.6	0.270	0.596	−0.326	2.19	4.87	−2.68
AuTe ($^2\Pi$)	2.518	2.750	0.232	54.7 (55.8)	10.2	0.170	0.517	−0.347	1.60	4.60	−3
AuF ($^1\Sigma^+$)	1.946	2.126	0.180	69.2	−10.6	0.674	0.877	−0.203	4.25	6.40	−2.15
AuCl ($^1\Sigma^+$)	2.248	2.454	0.206	64.9	−5.6	0.508	0.793	−0.285	3.69	6.44	−2.75
AuBr ($^1\Sigma^+$)	2.385	2.568	0.183	56.9	−8.1	0.452	0.749	−0.297	3.39	6.21	−2.82
AuI ($^1\Sigma^+$)	2.537	2.741	0.204	57.5	−1.3	0.347	0.678	−0.331	2.80	5.98	−3.18
HgH ($^2\Sigma^+$)	1.784 (1.749)	1.880	0.096	11.7 (9.5)	−10.4	0.332	0.530	−0.198	0.38	0.97	−0.59
HgO ($^3\Pi$)	2.231	2.223	−0.008	9.6	−17.5	0.416	0.688	−0.272	2.06	3.23	−1.17
HgS ($^3\Pi$)	2.600	2.602	−0.002	8.4	−14.7	0.341	0.595	−0.254	1.64	2.84	−1.2
HgSe ($^3\Pi$)	2.836	2.721	−0.115	6.0	−14.5	0.263	0.550	−0.287	1.43	2.58	−1.15
HgTe ($^3\Pi$)	2.970	2.933	−0.037	5.8	−10.5	0.222	0.485	−0.263	1.09	2.36	−1.27
HgF ($^2\Sigma^+$)	2.082	2.115	0.033	33.6	−29.2	0.665	0.862	−0.197	3.37	4.16	−0.79
HgCl ($^2\Sigma^+$)	2.461	2.495	0.034	22.6	−24.3	0.536	0.761	−0.225	3.04	4.10	−1.06
HgBr ($^2\Sigma^+$)	2.672	2.632	−0.040	16.1	−23.9	0.450	0.712	−0.262	2.87	3.90	−1.03
HgI ($^2\Sigma^+$)	2.820	2.842	0.022	13.6	−17.8	0.383	0.645	−0.262	2.34	3.71	−1.37
HgH^+ ($^1\Sigma^+$)	1.606 (1.597)	1.782	0.122	63.2	17.6	0.959	1.278	−0.319	0.30	1.94	−1.64
HgO^+ ($^2\Pi^+$)	1.997	2.127	0.130	24.0	−3.9	1.314	1.549	−0.235	2.22	4.20	−1.98
HgS^+ ($^2\Pi^+$)	2.343	2.473	0.130	45.5	9.5	0.991	1.307	−0.316	0.22	2.85	−2.63
$HgSe^+$ ($^2\Pi^+$)	2.488	2.590	0.102	47.3	9.9	0.889	1.214	−0.325	0.72	3.57	−2.85
$HgTe^+$ ($^2\Pi^+$)	2.668	2.791	0.123	57.3	18.6	0.740	1.089	−0.349	0.49	3.61	−3.12
HgF^+ ($^1\Sigma^+$)	1.943	2.023	0.080	38.2	−18.5	1.539	1.762	−0.223	3.73	5.70	−1.97
$HgCl^+$ ($^1\Sigma^+$)	2.274	2.380	0.106	43.0	−4.8	1.233	1.548	−0.315	2.17	4.85	−2.68
$HgBr^+$ ($^1\Sigma^+$)	2.428	2.508	0.080	41.2	−3.6	1.109	1.465	−0.356	2.56	5.47	−2.91
HgI^+ ($^1\Sigma^+$)	2.598	2.704	0.106	49.2	8.0	0.949	1.318	−0.369	2.21	5.49	−3.28

[(a)] Relat. and Non-relat denote results obtained at NESC/B3LYP and B3LYP, respectively. R(MX) gives the bond length of MX (M = Au, Hg, Hg^+), $\Delta R = R$(Non-relat) − R(Relat) the change in bond length due to scalar relativistic effects, BDE the bond dissociation energy, ΔE(Relat) = BDE(Relat) − BDE(Non-relat) the relativistic correction of the BDE, q(M) the charge transfer from M to X as calculated with NBO, Δq(M) = q(Relat) − q(Non-relat) the relativistic change in charge transfer, Dipole the dipole moment, and ΔDipole = Dipole(Relat) − Dipole(Non-relat) the relativistic change in the magnitude of the dipole moment. BDE values of the cations HgX^+ are given with regard to dissociation reaction (1): HgX^+ --> $Hg^+ + X$. - Numbers in parentheses denote experimental values taken from Refs. 2, 7, 78, 87.

similar electronegativities, we calculated in addition virial charges using zero-flux surfaces of the electron density distribution $\rho(\boldsymbol{r})$ and Bader's definition of atoms in molecules.[81] Molecular dipole moments were analyzed by determining charge transfer moments and atomic dipole moments. All calculations were carried out with the program packages COLOGNE08 (Ref. 82) and Gaussian03.[83]

RESULTS AND DISCUSSION

In Table 1, all calculated BDE values for molecules AuX, HgX and HgX^+ investigated in this work are summarized together with the corresponding bond lengths, dipole moments, and NBO charge transfer values. Table 2 lists some atomic properties of Au, Hg, and their bonding partners X.

Gold and mercury possess the electron configuration $[Xe]4f^{14}5d^{10}6s^1$ and $[Xe]4f^{14}5d^{10}6s^2$, respectively. Because of its preference for single bonding and the possibility of accepting negative charge, Au is considered sometimes as a pseudohalogen[7,84] or even as an analogue to hydrogen.[85] The latter is based on the fact that Au (2.54) and H (2.20) have about the same electronegativity (Table 2, Pauling scale). Bonding interactions in AuX and HgX are subject to large relativistic effects.[1,2,6,7] Therefore bonding has always to be discussed considering the influence of scalar relativistic effects.

The relativistic change in the molecular energy can lead to an increase in the BDE (positive relativistic correction ΔE(Relat)) or a decrease in the BDE of MX (negative ΔE(Relat)). In the former case the relativistic stabilization of the molecular energy is larger, in the latter case smaller than that of the sum of the relativistic atom stabilization energies for M and X. Relativity does not lead to significant energy changes for the first four periods of the periodic table. Also, relativistic changes are smaller for the fifth (Te, I) than the sixth period (Au, Hg), and since these changes are smaller for p than s-electrons, we assume that even for X = Te and I the relativistic energy lowering of M dominates.

If the charge of M in MX is larger (smaller) than that of the free atom M, the relativistic correction to the BDE should be positive (negative) leading to a stronger (weaker) bond. Any increase of the 6s population in the molecule *via* a charge transfer from X to M means an increase of the relativistic stabilization of M relative to that of the free atom M. This relationship is largely fulfilled when comparing NBO charge transfer values q(M) and relativistic corrections of the BDE, ΔE(Relat), of Table 1. The larger the positive charge at M in MX is (as a result of a large electronegativity of X), the more negative ΔE(Relat) becomes, *i.e.* the scalar relativistic correction leads to a weakening of the MX bond.

Table 2. Properties of Au, Hg, H, halogen, and chalcogen atoms[a]

Atom (State)	Pauling χ	IP1 exp / eV	NESC/HF orbital energies, ε / eV	Atomic, covalent radius, R / Å	Polarizability, α / Å^3
Au (^{2}S)	2.54	9.23	6.9 (6s) 18.1 (5d)	1.35, 1.44 (2.88)	6.48
Hg (^{1}S)	2.00	10.44	8.8 (6s) 16.3 (5d)	1.50, 1.49 (2.98)	5.7
Hg^+(^{2}S)	2.76[b]	18.76	13.1 (6s) 24.6 (5d)	1.27, 1.27 (2.54)	2.86[c]
H (^{2}S)	2.20	13.60	13.6 (1s)	0.25, 0.31 (1.75, 1.80)	0.67
F (^{2}P)	3.98	17.42	23.0 (pσ) 19.9 (pπ)	0.50, 0.71 (2.15, 2.20)	0.56
Cl (^{2}P)	3.16	12.97	15.8 (pσ) 13.7 (pπ)	1.00, 0.99 (2.43, 2.48)	2.18
Br (^{2}P)	2.96	11.81	14.3 (pσ) 12.4 (pπ)	1.15, 1.14 (2.58, 2.63)	3.05
I (^{2}P)	2.66	10.45	12.5 (pσ) 10.9 (pπ)	1.40, 1.33 (2.77, 2.82)	5.35
O (^{3}P)	3.44	13.62	19.3 (pσ) 16.6 (pπ)	0.60, 0.73 (2.17, 2.22)	0.80
S (^{3}P)	2.58	10.36	13.2 (pσ) 11.3 (pπ)	1.02, 1.96 (2.46, 2.51)	2.90
Se (^{3}P)	2.55	9.75	12.2 (pσ) 10.5 (pπ)	1.15, 1.16 (2.60, 2.65)	3.77
Te (^{3}P)	2.10	9.01	10.8 (pσ) 9.4 (pπ)	1.40, 1.35 (2.79, 2.84)	5.5

[a] Pauling electronegativities, atomic radii, and covalent radii from http://www.webelements.com, experimental first ionization potentials IP and polarizabilities α from Ref. 79; relativistic NESC/HF orbital energies ε were calculated for MX with M and X kept at a distance of 10 Å to enforce the symmetry of the MX molecule for the atoms. Values in parentheses give the ideal covalent AuX and HgX bond length estimated from covalent radii.

[b] Estimated on the basis of NBO charge transfer data in HgX^+ molecules.

[c] Taken from DK-CCSD(T) calculations: M. Ilias and P. Neogrady, *Chem. Phys. Lett*. **309** (1999) 441.

Interesting are the exceptions of these rule, which include a) some HgX^+ ions, b) AuX molecules with X having an electronegativity comparable or even smaller than that of Au, and c) the lower Au-chalcogenides. Before we discuss these molecules, we will first derive a simple molecular orbital (MO) model to analyze changes in bonding. In the previous section, we have given reasons why the SOC effect is not considered in

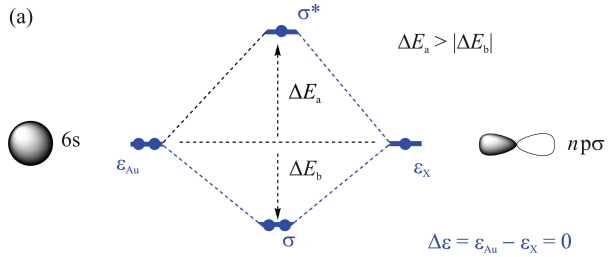

Figure 1a. Formation of σ-type bonding and antibonding MOs of AuX from 6s(Au) and pσ(X) AOs. Equal energies of the starting AOs are assumed, *i.e.* $\Delta\varepsilon = 0$. The energy difference between σ and σ* is given by $\Delta E = \Delta E_a + |\Delta E_b|$, the destabilization energy of the antibonding MO and the stabilization energy of the bonding MO.

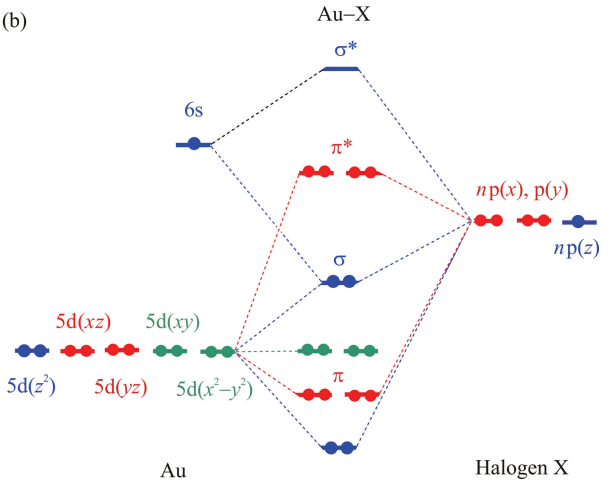

Figure 1b. Schematic MO diagram for the frontier MOs of MX. The diagram applies to the gold halides with the exception X = F. In the latter case, the σ MO is above the π* MOs.

this work. SOC leads to a change in the non-relativistic molecular orbitals (MOs), for example by mixing σ and π MOs. Therefore one has to ask whether it is justified to base a model for bonding in MX molecules on non-relativistic (or scalar relativistic) MOs. In this connection, we emphasize that trends in non-relativistic and relativistically corrected BDEs can be discussed based on such an MO model whereas the rationalization of second order effects introduced, for example, by SOC are not considered in this work.

The bonding model we will apply focuses on the formation of a set of σ/σ* MOs from 6s(M) and *n*pσ(X) and a set of π/π* MOs from 5d(M) and *n*pπ(X) as shown in the MO diagram of Figure 1b. The energy lowering ΔE_b (raising ΔE_a) of the bonding (antibonding) MO depends on the energy difference $\Delta\varepsilon$ of the AOs (the smaller $\Delta\varepsilon$, the larger the sum $|\Delta E_b| + \Delta E_a$, Figure 1a) and the orbital overlap S (the larger S, the larger $|\Delta E_b| + \Delta E_a$). Bond length reduction will increase S and change $\Delta\varepsilon$ in a way that can be anticipated by considering calculated AO energies calculated at the NESC/HF level or the first IPs of the atoms M and X (see Table 2) since trends in the experimental IPs give a qualitative measure for trends in the AO energies according to the Koopman theorem. However, it has to be considered that IPs for the halogens and chalcogens describe the removal of an electron from a doubly occupied *n*p orbital whereas for the MO diagram in Figure 1a distinction between *n*pσ and *n*pπ orbitals is required. For this purpose, we imposed the symmetry of MX on atoms M and X by calculating a stretched MX molecule with distance *R*(MX) = 10 Å. In this way, any significant electron interactions are suppressed, however *n*pσ and *n*pπ orbitals can be distinguished.

It has to be noted that the σ–σ* and π–π* energy difference $\Delta E = |\Delta E_b| + \Delta E_a$ is always dominated by the destabilization ΔE_a of the antibonding MO ($\Delta E_a > |\Delta E_b|$, Figure 1a) and therefore the occupation of the antibonding MO leads to a strong bond weakening effect. Hence, the 3-electron bonding situation of HgX molecules should lead to smaller BDE values than the 2-electron bonding situation of AuX and HgX^+ molecules. We will apply the MO model of Figure 1 when analyzing the changes in bond length and BDE values caused by the scalar relativistic effects. σ–π-Mixing caused by the SOC can make conclusions of a non-relativistic orbital model dubious. For the mercury chalcogenides, the influence of SOC on the BDEs was calculated to be smaller than 0.7 kcal mol^{-1} (Ref. 86) reflecting the fact that for molecules with occupied frontier orbitals of the σ-type (HgX and AuX) SOC plays energetically little role.

Relativistic Changes in Bond Lengths

The calculated NESC/B3LYP bond lengths are in good agreement with the few experimental values known today (Table 1, *R* values in parentheses). The relativistic shortening of *R*(MX) is documented by Δ*R* in Table 1. It can be increased or reduced in dependence of other electronic effects. If two electrons occupy the 6s-orbital, Coulomb and exchange repulsion between M and X should be larger and accordingly Δ*R* should be smaller. Hence, bond shortening should be larger for AuX than for HgX, which is confirmed for AuH and HgH. Charge transfer is another effect that can influence the magnitude of Δ*R*. The electronegativity of X will influence the degree of charge transfer. If negative charge is withdrawn from the 6s orbital of M in molecule MX, the remaining 6s charge will be less shielded and more attracted to the nucleus, *i.e.* the relativistic 6s orbital contraction is complemented by a non-relativistic contraction and the MX bond becomes stronger. However, charge transfer will also be influenced by the length of

the bond in the way that the relativistic shortening of the bond leads to reduced charge transfer, less ionic character of the bond, and a decrease in bond strength. This non-relativistic effect dominates charge transfer; it is complemented by a smaller relativistic reduction of charge transfer caused by orbital contraction. The relativistic shortening of the bond leads to both strengthening and weakening of the bond where the former effect will dominate (if no other effects play a role) with the result that R becomes shorter. However, reduction of the ionic character as indirectly caused by relativity prevents a too large value of ΔR.

There are several other effects that also hinder relativistic bond shortening ΔR as caused by an increase of the stabilizing mass-velocity effect for smaller R.[2,9] Lone pair repulsion between M and X increases when the bond shortens and therefore should imply smaller ΔR values. For the halogens, lone pair repulsion in MX becomes larger than for the chalcogens because of 4 rather than 3 pπ electrons at X, which explains that ΔR values are smaller for the former when compared to the latter (Table 1, AuF: 0.180 *vs* AuO: 0.281 Å).

Besides lone pair repulsion, increased nuclear repulsion can also hinder relativistic bond shortening. The HgX^+ ions are lacking one electron and since this leads to stronger nuclear repulsion between Hg and X, the ΔR values are smaller than those for the isoelectronic AuX molecules by 0.10 to 0.15 Å (Table 1).

Another effect hindering a relativistic bond length contraction is the subsequent increase in antibonding character. In neutral HgX, the σ* MO is occupied by one electron (Figure 1). Any bond length reduction raises the energy of this MO thus weakening the HgX bond and leading to an overall destabilization of the molecule. The ΔR values of the neutral mercury halides are rather small (0.022 to 0.033 Å, Table 1) thus confirming that a strong σ* MO-effect leads to a smaller relativistic bond length contraction.

An even stronger effect that hinders relativistic bond shortening is exchange repulsion. The neutral mercury chalcogenides possess a $^3\Pi$ state as ground state (occupation of π* and σ* MOs by 3 and 1 electron, respectively), in which one of the two unpaired α-electrons is preferentially at Hg, the other preferentially at the chalcogen atom. A longer bond reduces exchange repulsion and the antibonding effect of the σ* MO. Since the orbital contraction reduces charge transfer from Hg to X and lowers by this the ionic character of the mercury-chalcogenide bond, it is weakened compared to the non-relativistic situation and becomes even longer (negative ΔR values in Table 1).

Selenium and bromine take an exceptional position in the comparison of the HgX molecules, as the corresponding ΔR values are both negative (−0.115 and −0.040 Å, *i.e.* lengthening of the bond due to relativity; Table 1) and relatively large in magnitude. They differ clearly from the general trends in ΔR values obtained for the Hg-chalcogenides and Hg-halides, respectively. This is a reflection of the d-block contraction effect known to be active for Ga, Ge, As, Se, and Br.[87] Incomplete shielding of the nucleus by the d-electrons leads to stronger contraction of the atomic density, a smaller covalent radius, and a larger electronegativity than expected for these atoms on the basis of the trends in the corresponding group (Table 2). Consequently, reduction of the ionic character is stronger than for the other members of the chalcogen or halogen group (Table 2, −0.287 and −0.262 electron) and relativity leads to bond weakening.

Relativistic Changes in the Bond Strength

A relativistic shortening of the bond length does not necessarily imply an increase in the bond strength. On the contrary, the molecular stability and the bond strength depend on the negative charge in the 6s orbital and its stabilization by scalar relativistic effects. In view of the electronegativity values for M and X, there is in most cases a reduction of negative charge in the 6s orbital and therefore a relativistically caused decrease in bond strength despite the shortening of the bond (Table 1). There are however also exceptions to this rule as was mentioned above.

In the case of the HgX^+ ions, NBO charges suggest that the positive charge is largely localized at Hg. Accordingly, the BDE values correspond to a dissociation into $Hg^+(^2S) + X$ rather than $Hg(^1S) + X^+$. If in the molecule the charge at Hg is smaller than +1, the relativistic stabilization will become larger than in free Hg^+ and ΔE(relat) turns out to be positive. This situation is given for HgH^+, HgS^+, $HgSe^+$, $HgTe^+$, and HgI^+ (Table 1).

For AuX molecules with X being equally or more electropositive than Au (X = H, Se, Te, Table 2), a positive NBO charge at the metal atom is calculated (Table 1). Calculation of the virial charges in these cases, however, leads to charge transfer from X to A and a negatively charged Au atom (see below), which means that the relativity effect increases for the molecule relative to that of the free metal atom and leads in this way to a stronger AuH, AuSe, or AuTe bond thus explaining the positive ΔE(Relat) values of 22.7, 6.6, and 10.8 kcal mol^{-1} (Table 1). We draw from this the conclusion that the NBO charges exaggerate charge transfer from M to X and therefore they are not reliable in the case of comparable electronegativities. Virial charges lead to a more realistic description of the charge distribution and, accordingly, predictions of stability changes caused by relativity are better based on them.

It remains to clarify the relativistic increase in bond strength for AuO and AuS. In these cases, the relativistic bond shortening ΔR is unusually large (0.281, and 0.257 Å, Table 1), which is due to the fact that the σ* MO is not occupied, lone-pair repulsion is reduced, and none of the other bond lengthening effects mentioned above plays any role. The relativistic R values (1.88 and 2.21 Å, Table 1) are significantly shorter than the sum of the covalent radii of the corresponding atoms (Table 2). In the molecule, there is more negative charge in a volume defined by the free Au atom (radius 1.44 Å, Table 2) so that the relativistic stabilization increases from the free M atom to the molecule. Similar effects are found for all AuX molecules (Tables 1 and 2) so that ΔE(Relat) values become more positive than for HgX and HgX^+ where however this effect becomes smaller with increasing atomic number of X.

Bonding in AuH, HgH^+ and HgH

For AuH, NESC/B3LYP leads to a bond length of 1.535 Å and a BDE of 74.2 kcal mol^{-1}, which are in reasonable agreement with experimental values of 1.528 Å[88] and 74.3 kcal mol^{-1}.[88] There is a large number of quantum chemical investigations on AuH[8–16] (for a recent summary see Ref. 7) and therefore we will focus here just on AuH bonding. According to calculated NBO charges, 0.072 electrons are transferred from Au to H and the calculated dipole moment (1.4 Debye) is oriented from H (negative end) to Au (positive end, physical notation) despite Pauling electronegativities of 2.20 (H) and 2.54 (Au), respectively (Table 2).

Bonding is provided preferentially by the σ-MO shown in Figure 1. Because of the lack of any π–electrons at hydrogen, lone pair repulsion cannot play any role. The scalar relativistic effect on the BDE is 22.7 kcal mol^{-1}, *i.e.* the non-relativistic BDE is just 51.5 kcal mol^{-1} at a bond length of 1.746 Å, which is 0.210 Å longer than the relativistic value (Table 1). The relativistic contraction of the 6s(Au) orbital lowers the energy of this orbital and charge transfer from Au to H is reduced from 0.445 to 0.072 electron where most of this change is caused by the relativistic bond contraction (Table 1). The polar character of the bond is reduced and the AuH bond should be weakened, which is contrary to the increase of the BDE value. As mentioned above, the NBO charges are obviously misleading.

For HgH^+, effects are similar as reflected by a relativistic BDE of 63.2 kcal mol^{-1} due to a relativistic increase of 17.6 kcal mol^{-1}. Reduced shielding of the nucleus caused by the positive charge of the ion leads to somewhat weaker bonding and a bond length of 1.606 Å (non-relativistic: 1.782 Å, Table 1), which according to the difference in covalent radii for Au and Hg should be at 1.59 Å (1.54 + 0.05, Tables 1 and 2). As soon as the σ* MO is occupied by a single electron as in HgH, the stronger orbital interactions caused by the scalar relativistic effects lower the energy of the σ MO and raise the σ* energy, where the destabilizing effect outweighs the stabilizing effect and leads to an overall weakening of the HgH bond. The BDE is reduced from 21.2 by 9.5 to 11.7 kcal mol^{-1}. The overall destabilization of the bond by the extra electron in the σ* MO is more than 50 kcal mol^{-1}, which is suggested when comparing the BDE values of HgH and HgH^+.

It is noteworthy that the AuH, HgH and HgH^+ dipole moments are directed in the same way as those of other AuX (HgX) molecules investigated in this work, however the former are considerably smaller than the latter (Table 1). The total molecular dipole moment depends on both the charge transfer moment and the atomic dipole moments (Figure 2). The charge transfer moment is determined by the amount of charge transferred from Au (Hg) to X and the AuX (HgX) bond length. Its orientation is opposite to the direction of charge transfer. Transfer from Au (Hg) to X leads to an anisotropic charge distribution at the metal atom M: charge is depleted on the bond side of M and accumulated in front of X (situation of HgH^+: regions of depletion and accumulation of negative charge are schematically indicated in Figure 2 by empty and filled ellipses; Figure 2c). Charge polarization in the bond leads to accumulation of electron density on the non-bonded side of M, but to a depletion of charge on the non-bonded side of X as indicated in Figure 2 for HgH^+. The atomic dipole moments are mostly oriented opposite to the charge transfer moment and lead to a total moment smaller than the charge transfer moment. However, in the case of a small charge transfer moment (small charges, relatively small distance) and relatively large atomic dipole moments (large volume, large polarizability of the atoms), the molecular dipole moment can be dominated by the atomic dipole moments and therefore it takes the opposite direction than the charge transfer moment.

This is the case of the dipole moment of AuH where the calculated virial charges (q(Au) = −0.040 electron, Figure 2) are in line with the electronegativities of Table 2 thus disproving the NBO charges (q(Au) = 0.075 electron, Table 1). The charge transfer moment is −0.295, the atomic dipole moments 1.171 (Au) and 0.513 Debye (H) thus leading to a total dipole moment of −0.295 + 1.685 = 1.390 Debye in good agreement with the wave function dipole moment of 1.392 Debye.

In the case of HgH, the charge transfer moment is oriented in the opposite way and larger (longer distance, larger charges, Table 1) because of the significant charge transfer from Hg to H (virial charge: −0.137 electron, Figure 2). The atomic dipole moments are

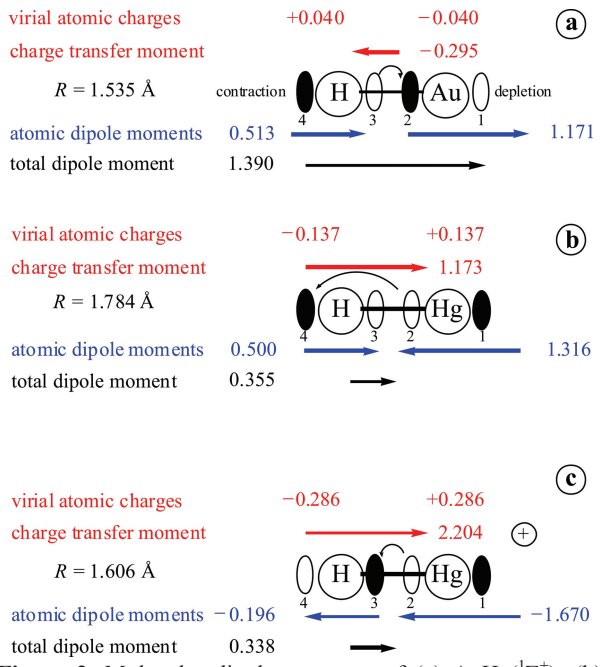

Figure 2. Molecular dipole moments of (a) AuH ($^1\Sigma^+$); (b) HgH ($^2\Sigma^+$); and (c) HgH^+ ($^1\Sigma^+$). Charge transfer moment (red), atomic dipole moments (blue), and total dipole moment (black) are given in Debye units, each symbolized by an arrow where the arrowhead points to the positive end of the dipole. Virial charges (in electron) and bond lengths (in Å) for the calculation of the charge transfer moments are also given. Regions of charge depletion and charge accumulation inside the bond (2,3) and outside the bond (1,4) are given by empty and filled ellipses. A curved black arrow gives the direction of charge transfer. NESC/B3LYP calculations.

opposite to each other. The Hg dipole moment follows the direction of the charge transfer and the normal depletion-contraction pattern of the atomic density (Figure 2). Since the total electron density of Hg is a factor 80 higher than that of H, the density of the latter atom is strongly enhanced by the tail density of the former so that charge transfer from Hg to H leads to an increase of the density at the non-bonded side of H (schematically shown in Figure 2). The atomic dipole moment of H is opposite to that of Hg. The sum of the atomic dipole moments becomes somewhat smaller than the value of the charge transfer moment and reduces the latter to the rather small value of 0.36 Debye (Figure 2). A similar situation applies to HgH^+, *i.e.* again transfer moment and atomic dipole moments are oriented oppositely and cancellation leads to a rather small total dipole moment of 0.34 Debye.

Bonding in Gold Halides, Mercury Halides, and Mercury Halide Cations

According to NESC/B3LYP calculations, the gold halides AuX possess BDE values between 69 (X = F) and 57 kcal mol^{-1} (X = Br or I) where the total relativistic energy corrections increase from −10.6 to −1.3 kcal mol^{-1} (Table 1). Similar values are reported in the literature.[24–34] For AuF, charge transfer from Au to F is, despite a substantial relativistic reduction, largest for all Au-halides and accordingly AuF should have the strongest ionic contribution to bonding. In the case of AuI, 6s and *n*pσ orbital should interact stronger (ε(6s) is energetically closer to ε(I,pσ) than ε(F,pσ), Table 2) than in the case of the lower halogens thus leading to a significant stabilization of the bonding σ MO where however π-repulsion should cancel this effect largely.

Different trends are found for the isoelectronic mercury halide cations. Their BDE values increase from 38 (X = F) to 49 kcal mol^{-1} (X = I, Table 1). The corresponding relativistic corrections increase from −18 to 8 kcal mol^{-1}. As mentioned above, these trends result partly from the fact that due to relativity negative charge is transferred back to the halogen thus leading in the case of X = I to an increase of negative charge by more than 0.3 electron (Table 1) relative to that of free Hg^+ thus increasing relativistic stabilization in MX relative to the separated atoms. One could also argue (as in the case of the Au-halides) that a decrease in ionic bonding with increasing atomic number of X should actually weaken the HgI^+ bond. There is however a significant nuclear repulsion, which a) reduces ΔR (see above) and b) increases from I to F according to relativistic bond lengths of 2.598 (HgI^+) and 1.943 Å (HgF^+, Table 1) thus reverting the trend in BDEs from the Au-halides to the Hg-halide cations.

For the mercury halides, occupation of the energetically destabilized σ* MO in combination with a decrease in ionic bonding is decisive for the calculated trend in BDEs (HgF: 33.6; HgI: 13.6 kcal mol^{-1}, Table 1). The latter effect leads to the same decrease in the BDEs from X = F to X = I as found for the Au-halides. However, this trend is enlarged by the σ*-effect. Destabilization of the σ* MO increases with the increasing covalent character of the HgX bond is, which requires similar energies of the atomic orbitals involved in bonding. According to the calculated orbital energies, 6s(Hg) and 5pσ(I) have energies just 2 eV apart (Table 2) and the σ–σ* energy difference should be largest for HgI, which implies strong destabilization of the molecule due to single occupation of the σ* MO. Hence, the HgI bond should be strongly weakened relative to the HgF bond thus enlarging the trend due to the changes in ionic bonding, which is confirmed by the NESC/B3LYP results.

Bonding in Gold Chalcogenides, Mercury Chalcogenides, and Mercury Chalcogenide Cations

The BDEs of Au-chalcogenides AuE (E: chalcogen) are comparable in magnitude to those of the corresponding

halides and show also some irregularities when increasing the atomic number of X (53, 60, 54, 55 kcal mol^{-1}, Table 1). Calculated values agree reasonably with experimental values of 53.7, 59.7, 57.2, and 55.8 kcal mol^{-1} (Refs. 79 and 88) (Table 1) and results of previous investigations.[17–23] Although ionic bonding should be smaller compared to the Au-halides, there is the possibility of reduced lone pair repulsion and some residual π-bonding (π-effect) according to a occupation of the π* MOs with 3 rather than 4 electrons. The relativistic stabilization of the σ-MO should be largest for Te (IP values of 9.0 and 9.2 for Au and Te, Table 2) whereas the π-effect should be strongest for S (ε-values for 5d(Au) and 3pπ(S), Table 2). This is in line with the calculated BDE values.

In the case of the Hg-chalcogenide cations, nuclear repulsion weakens the HgO bond (1.997 Å) more than the HgTe bond (2.668 Å, Table 1) thus leading to increased BDE values with increasing atomic number of E (increase from 24 to 57 kcal mol^{-1}). This trend is supported by the increase in electronic charge at the Hg atom in HgE^+ (+0.31, −0.01, −0.11, −0.26 relative to +1 electron in free Hg^+, Table 1), which enhances the relativistic stabilization of the HgE^+ ions.

The two lowest states of the mercury chalcogenides are $^3\Pi$ and $^1\Sigma^+$, where the first state is just a couple of kcal mol^{-1} below the second state.[35,36] The larger stability of the $^3\Pi$ states is the result of a number each other balancing electronic effects as has been discussed in the literature.[35] Occupation of the σ* orbital and subsequent destabilization, the residual π-bonding effect replacing lone pair repulsion, reduced charge transfer and reduced ionic bonding, replacement of Coulomb repulsion by exchange repulsion, and at the same time bond lengthening due to a much smaller relativistic bond length contraction, all these effects play a role and lead to a somewhat larger stabilization of $HgE(^3\Pi)$. On the basis of the bonding model used in this work, it is difficult to predict which state is more stable and how the BDE values should change with increasing atomic number of E. Occupation of the σ* MO and the relatively long relativistic *R* values explain the low BDEs, which vary by just 3 kcal mol^{-1} from 6 (E = Te) to 9 kcal mol^{-1} (E = O, Table 1).

CONCLUSION

This work has shown that NESC in combination with B3LYP leads to a reasonable description of AuX, HgX, and HgX^+ (X = H, halogen, chalcogen) molecules and their bonding properties. AuX bonding is substantially stronger than HgX bonding, which is simply a result of the additional 6s electron in Hg and the creation of a 3-electron bonding situation, which leads to strongly reduced BDEs.

The dependence of AuX and HgX bonding on relativity has been discussed considering several electronic effects that determine the strength of the MX bond (relativistic 6s-electron effect, charge transfer effect (ionic bonding), σ*-effect, lone pair repulsion effect, residual π-bonding, and d-block effect). Relativistic effects are especially strong in the case of Au (*gold maximum*)[2,7] and somewhat weaker in the case of Hg. There is a complex interplay between charge transfer (ionic bonding) and relativity. If charge transfer leads to a decrease of the 6s electron density, the relativistic lowering of the energy is smaller for the molecule than the free atom M (Au or Hg) and the BDE is reduced. This effect is outweighed because charge transfer increases ionic bonding, which leads to a strengthening of the bond. Bond length reduction and orbital contraction adjusts these effects so that less charge is transferred and relativistic stabilization becomes larger. The magnitude of the BDE depends on how much charge is transferred, the degree of σ-bonding, the magnitude of the lone pair effect, and how much other electronic effects contribute to bonding.

Relativistic changes in the BDE of AuX and HgX are always negative apart from a few exceptional cases. An increase in the BDE upon including scalar relativistic effects is found when charge transfer occurs from X to M due to the low electronegativity of X. This work has shown that virial charges are more reliable than NBO charges to determine the direction of charge transfer. Virial partitioning of the electron density distribution helps to rationalize relativistic influences on orientation and magnitude of molecular dipole moments.

Relativistic BDEs reflect also the magnitude of the bond length reduction Δ*R* caused by the mass-velocity contribution. The various electronic effects influencing the magnitude of Δ*R* have been identified and used to explain unusually short (*e.g.*, gold chalcogenides) and unusually long relativistic bond lengths *R* (mercury chalcogenides). Effects that play a role in this connection are the σ*-effect (occupation of an antibonding, destabilized MO) and the lone pair repulsion effect. The magnitude of these effects can be estimated using calculated orbital energies of the free atoms M and X to qualitatively predict the energy difference between bonding and antibonding (σ or π) MOs.

We have shown that a bonding model based on non-relativistic MOs can be useful to describe relativistic effects. Of course, one has always to consider relativistic effects that can change orbital properties. For example, SOC can lead to a mixing of σ and π MOs thus altering the nodal properties, orbital overlap, and orbital

energy. Therefore, we have i) avoided in this work to refer to overlap and nodal properties and ii) used NESC/HF orbital energies to confirm calculated trends. The bonding model developed in this work can be applied to other mercury and gold compounds. Work is in progress to test its advantages and its range of applications.

Acknowledgements. EK and DC thank the National Science foundation and the University of the Pacific for financial support. Preliminary calculations were carried out by F. Axe.

REFERENCES

1. S. J. Rose, I. P. Grant, and N. C. Pyper, *J. Phys. B* **11** (1978) 1171−1176.
2. P. Pyykkö, *Chem. Rev*. **88** (1988) 563−594.
3. H. Schmidbaur (Ed.), *Gold. Progress in Chemistry, Biochemistry and Technology*, Wiley, Chichester, 1999, p. 894.
4. P. Pyykkö, *Relativistic Theory of Atoms and Molecules*, Vol. III, Springer, Berlin, 2000, pp. 108−111.
5. H. Schwarz, *Angew. Chem*. **115** (2003) 4580−4593; *Angew. Chem. Int. Ed*. **42** (2003) 4442−4454.
6. P. Schwerdtfeger, *Angew. Chem*. **115** (2003) 1936−1939; *Angew. Chem. Int. Ed*. **42** (2003) 1892−1895.
7. P. Pyykkö, *Angew. Chem. Int. Ed*. **43** (2004) 4412−4456.
8. P. J. Hay, W. R. Wadt, L. R. Kahn, and F. W. Bobrowicz, *J. Chem. Phys*. **69** (1978) 984−997.
9. T. Ziegler, J. G. Snijders, and E. J. Baerends, *Chem. Phys. Lett.* **75** (1980) 1−4.
10. G. Jansen and B. A. Hess, *Z. Phys. D* **13** (1989) 363−375.
11. O. D. Häberlen and N. Rösch, *Chem. Phys. Lett*. **199** (1992) 491−496.
12. E. van Lenthe, E. J. Baerends, and J. G. Snijders, *J. Chem. Phys*. **101** (1994) 9783−9792.
13. E. van Lenthe, J. G. Snijders, and E. J. Baerends, *J. Chem. Phys*. **105** (1996) 6505−6516.
14. R. Franke and C. van Wüllen, *J. Comput. Chem*. **19** (1998) 1596−1603.
15. T. Tsuchiya, M. Abe, T. Nakajima, and K. Hirao, *J. Chem. Phys*. **115** (2001) 4463−4472.
16. P. Schwerdtfeger, J. R. Brown, J. K. Laerdahl, and H. Stoll, *J. Chem. Phys*. **113** (2000) 7110−7118.
17. A. Citra and L. Andrews, *J. Mol. Struct. (Theochem)* **489** (1999) 95−108.
18. L. C. O'Brien, A. E. Oberlink, and B. O. Roos, *J. Phys. Chem. A* **110** (2006) 11954−11957.
19. T. Ichino, A. J. Gianola, D. H. Andrews, and W. C. Lineberger, *J. Phys. Chem. A* **108** (2004) 11307−11313.
20. T. Okabayashi, F. Koto, K. Tsukamoto, E. Yamazaki, and M. Tanimoto, *Chem. Phys. Lett.* **403** (2005) 223−227.
21. S. Shaji, A. Song, J. J. O'Brien, B. A. Borchert, and L. C. O'Brien, *J. Mol. Spectrosc*. **243** (2007) 37−42
22. Z. J. Wu, *J. Phys. Chem. A* **109** (2005) 5951−5955.
23. J. M. Seminario, A. G. Zacarias, and J. M. Tour, *J. Am. Chem. Soc*. **121 (**1999) 411.
24. (a) P. Schwerdtfeger, J. S. McFeaters, R. L. Stephens, M. J. Liddell, M. Dolg, and B. A. Hess, *Chem. Phys. Lett*. **218** (1994) 362−366; (b) P. Schwerdtfeger, J. S. McFeaters, M. J. Liddell, J. Hrusák, and H. Schwarz, *J. Chem. Phys.* **103** (1995) 245−252.
25. (a) M. Mayer, O. D. Häberlen, and N. Rösch, *Phys. Rev. A* **54** (1996) 4775−4782; (b) V. A. Nasluzov and N. Rösch, *Chem. Phys. Lett*. **210** (1996) 413−425.
26. J. K. Laerdahl, T. Saue, and K. Faegri, Jr., *Theor. Chem. Acc*. **97** (1997) 177−184.
27. M. Ilia, P. Furdík, and M. Urban, *J. Phys. Chem. A* **102** (1998) 5263−5268.
28. C. van Wüllen, *J. Chem. Phys.* **109** (1998) 392−399.
29. P. Alemany, L. Bengtsson-Kloo, and B. Holmberg, *Acta Chem. Scand.* **52** (1998) 718−727.
30. K. G. Dyall and T. Enevoldsen, *J. Chem. Phys*. **111** (1999) 10000−10007.
31. W.-J. Liu and C. van Wüllen, *J. Chem. Phys*. **110** (1999) 3730−3735.
32. Y.-K. Han and K. Hirao, *Chem. Phys. Lett*. **324** (2000) 453−458.
33. T. Söhnel, R. Brown, L. Kloo, and P. Schwerdtfeger, *Chem. Eur. J*. **7** (2001) 3167−3173.
34. M. Guichemerre, G. Chambaud, and H. Stoll, *Chem. Phys*. **280** (2002) 71−102.
35. M. Filatov and D. Cremer, *ChemPhysChem*. **5 (**2004) 1547−1557.
36. B. C. Shepler and K. A. Peterson, *J. Phys. Chem. A* **107 (**2003) 1783−1787.
37. B. C. Shepler, N. B. Balabanov, and K. A. Peterson, *J. Chem. Phys*. **127 (**2007) 164304−164310.
38. B. C. Shepler, A. D. Wright, N. B. Balabanov, and K. A. Peterson, *J. Phys. Chem. A* **111** (2007) 11342−11349.
39. K. A. Peterson, B. C. Shepler, and J. M. Singleton, *Mol. Phys*. **105 (**2007) 1139−1155.
40. B. C. Shepler, N. B. Balabanov, and K. A. Peterson, *J. Phys. Chem. A* **109** (2005) 10363−10372.
41. N. B. Balabanov, B. C. Shepler, and K. A. Peterson, *J. Phys. Chem. A* **109** (2005) 8765−8773.
42. N. B. Balabanov and K. A. Peterson, *J. Chem. Phys.* **120** (2004) 6585−6592.
43. N. B. Balabanov and K. A. Peterson, *J. Chem. Phys.* **119** (2003) 12271−12278.
44. N. B. Balabanov and K. A. Peterson, *J. Phys. Chem. A* **107** (2003) 7465−7470.
45. J. A. Tossell, *J. Phys. Chem. A* **110** (2006) 2571−2578.
46. J. A. Tossell, *J. Phys. Chem. A* **107** (2003) 7804−7091.
47. J. A. Tossell, *J. Phys. Chem. A* **105** (2000) 935−946.
48. J. A. Tossell, *Am. Mineral.* **84** (1999) 877−883.
49. J. A. Tossell, *J. Phys. Chem. A* **102** (1998) 3587−3591.
50. M. E. Goodsite, J. M. Plane, and H. Skov, *Environ. Sci. Technol.* **38** (2004) 1772−1786.
51. A. F. Khalizov, B. Viswanathan, P. Larregaray, and P. A. Ariya, *J. Phys. Chem. A* **107** (2003) 6360−6365.
52. A. Hu, P. Otto and J. Ladik, *J. Mol. Struct.* **468** (1999) 163−168.
53. (a) T. R. Cundari and E. W. Moody, *Mol. Struct.* **425** (1998) 43−50; (b) M. Kaupp and H. G. von Schnering, *Inorg. Chem.* **33** (1994) 2555−2564.
54. M. Liao, Q. Zhang, and W. H. E. Schwarz, *Inorg. Chem.* **34** (1995) 5597−5605.
55. V. Barone, A. Bencini, T. Federico, and M. G. Uytterhoeven. *J. Phys. Chem.* **99** (1995) 12743−12750.
56. S. T. Howard, *J. Phys. Chem.* **98** (1994) 6110−6113.
57. M. Kaupp, M. Dolg, H. Stoff, and H. J. v. Schnering, *Inorg. Chem*. **33** (1994) 2122−2131.
58. P. P. D. Schwerdtfeger, W. Boyd, S. Brieen, J. S. McFeaters, M. Dolg, M. S. Liao, and E. W. H. Schwarz, *Inorg. Chim. Acta* **213** (1993) 233−246.
59. D. Stromberg, O. Gropen, and U. Wahlgren, *Chem. Phys.* **133** (1989) 207−219.
60. (a) E. van Lenthe, E. J. Baerends, and J. G. Snijders, *J. Chem. Phys*. **99** (1993) 4597−4610; (b) E. van Lenthe, E. J. Baerends, and J. G. Snijders, *J. Chem. Phys*. **101** (1994) 9783−9792.
61. (a) K. G. Dyall and E. van Lenthe, *J. Chem. Phys*. **111** (1999) 1366−1372; (b) E. van Lenthe, A. Ehlers, and E. J. Baerends, *J. Chem. Phys*. **110** (1999) 8943−8953.

62. M. Filatov and D. Cremer, *J. Chem. Phys*. **122** (2005) 044104-044108.
63. (a) M. Filatov and D. Cremer, *Mol. Phys*. **101** (2003) 2295−2302; (b) M. Filatov and D. Cremer, *J. Chem. Phys*. **119** (2003) 1412−1420; (c) M. Filatov and D. Cremer, *J. Chem. Phys*. **119** (2003) 701−712.
64. M. Filatov and D. Cremer, *J. Chem. Phys*. **118** (2003) 6741−6750.
65. (a) M. Filatov and D. Cremer, *Theor. Chem. Acc*. **108** (2002) 168−178; (b) M. Filatov and D. Cremer, *Chem. Phys. Lett*. **351** (2002) 259−266; (c) M. Filatov and D. Cremer, *Chem. Phys. Lett.* **370** (2003) 647−653.
66. M. Filatov and D. Cremer, *J. Chem. Phys*. **122** (2005) 06410-4-06410-8.
67. K. G. Dyall, *J. Chem. Phys*. **106** (1997) 9618−9626.
68. M. Filatov and K. G. Dyall, *Theor. Chem. Acc*. **117** (2007) 333−338.
69. E. Kraka and D. Cremer, *Int. J. Mol. Sci*. **9** (2008) 926−942.
70. D. Cremer, E. Kraka, and M. Filatov, *Chem. Phys. Chem.* **9** (2008) 2510−2521.
71. K. Raghavachari, G. W. Trucks, J. A. Pople, and M. Head-Gordon, *Chem. Phys. Lett.* **157** (1989) 479−483.
72. W. Kohn and L. J. Sham, *Phys. Rev*. **140** (1965) A1133−A1138.
73. A. D. Becke, *J. Chem. Phys*. **98** (1993) 5648−5652.
74. A. D. Becke, *Phys. Rev. A* **38** (1988) 3098−3100.
75. C. Lee and W. Yang, *Phys. Rev. B* **37** (1988) 785−789.
76. (a) Au, Hg and K: G. Dyall, *Theor. Chem. Acc.* **112** (2004) 403−409; (b) Te, I and K: G. Dyall, *Theor. Chem. Acc.* **115** (2006) 441−447.
77. S. F. Boys and F. Bernardi, *Mol. Phys.* **19** (1970) 553−566.
78. (a) T. H. Dunning, Jr., *J. Chem. Phys.* **90** (1989) 1007−1023; (b) D. E. Woon and T. H. Dunning, Jr., *J. Chem. Phys.* **98** (1993) 1358−1371; (c) D. E. Woon, and T. H. Dunning, Jr., *J. Chem. Phys*. **100** (1994) 2975; (d) A. K. Wilson, D. E. Woon, K. A. Peterson, and T. H. Dunning, Jr., *J. Chem. Phys.* **110** (1999) 7667−7676.
79. D. R. Lide (Ed.), *Handbook of Chemistry and Physics,* 72nd Edition, CRC Press, Boca Raton, 1992.
80. E. Reed, L. A. Curtiss, and E. Weinhold, *Chem. Rev*. **88** (1988) 899−926.
81. R. F. W. Bader, *Atoms in Molecules, A Quantum Theory*, Clarendon Press, Oxford, 1994.
82. E. Kraka, J. Gräfenstein, M. Filatov, H. Joo, D. Izotov, J. Gauss, Y. He, A. Wu, V. Polo, L. Olsson, Z. Konkoli, Z. He, and D. Cremer, COLOGNE08. University of Pacific, Stockton, CA, 2008.
83. M. J. Frisch, G. W. Trucks, H. B. Schlegel, G. E. Scuseria, M. A. Robb, J. R. Cheeseman, J. A. Montgomery, Jr., T. Vreven, K. N. Kudin, J. C. Burant, J. M. Millam, S. S. Iyengar, J. Tomasi, V. Barone, B. Mennucci, M. Cossi, G. Scalmani, N. Rega, G. A. Petersson, H. Nakatsuji, M. Hada, M. Ehara, K. Toyota, R. Fukuda, J. Hasegawa, M. Ishida, T. Nakajima, Y. Honda, O. Kitao, H. Nakai, M. Klene, X. Li, J. E. Knox, H. P. Hratchian, J. B. Cross, V. Bakken, C. Adamo, J. Jaramillo, R. Gomperts, R. E. Stratmann, O. Yazyev, A. J. Austin, R. Cammi, C. Pomelli, J. W. Ochterski, P. Y. Ayala, K. Morokuma, G. A. Voth, P. Salvador, J. J. Dannenberg, V. G. Zakrzewski, S. Dapprich, A. D. Daniels, M. C. Strain, O. Farkas, D. K. Malick, A. D. Rabuck, K. Raghavachari, J. B. Foresman, J. V. Ortiz, Q. Cui, A. G. Baboul, S. Clifford, J. Cioslowski, B. B. Stefanov, G. Liu, A. Liashenko, P. Piskorz, I. Komaromi, R. L. Martin, D. J. Fox, T. Keith, M. A. Al-Laham, C. Y. Peng, A. Nanayakkara, M. Challacombe, P. M. W. Gill, B. Johnson, W. Chen, M. W. Wong, C. Gonzalez, and J. A. Pople, *Gaussian 03*, Revision C.02, Gaussian, Inc., Wallingford CT, 2004.
84. M. Jansen and A. V. Mudring, in: H. Schmidbaur (Ed.), *Gold. Progress in Chemistry, Biochemistry and Technology,* Wiley, New York, 1999, pp. 747−793.
85. J. W. Lauher and K. Wald, *J. Am. Chem. Soc*. **103** (1981) 7648−7650.
86. K. A. Peterson, B. C. Shepler, and J. M. Singleton, *Mol. Phys.* **105** (2007) 1139−1155.
87. N. N. Greenwood and A. Earnshaw, *Chemistry of the Elements*, 2nd Edition, Butterworth-Heinemann, Oxford, 1997.
88. K. P. Huber and G. Herzberg, *Molecular Spectra and Molecular Structure IV. Constants of Diatomic Molecules*, Van Nostrand Reinhold, New York, 1979.

SAŽETAK

Usporedba kemijskog vezanja zlata i žive

Elfi Kraka,[a] Michael Filatov[b] i Dieter Cremer[a]

[a]*Department of Chemistry, University of the Pacific, 3601 Pacific Avenue, Stockton, CA 95211, USA*
[b]*Department of Chemistry, Zernike Institute for Advanced Materials, University of Groningen, Nijenborgh 4, 9747AG Groningen, Netherlands*

Proučavano je devet AuX molekula (X = H, O, S, Se, Te, F, Cl, Br, I), njihovih izoelektronskih HgX^+ analoga i odgovarajućih neutralnih dvoatomnih HgX molekula upotrebom NESC (Normalized Elimination of the Small Component) i B3LYP teorije kako bi se odredio utjecaj relativističkih efekata na energije disocijacije veze (BDE), duljine kemijskih veza, dipolne momente i raspodjelu atomskih naboja. Relativistički efekti znatnije su veći za AuX nego za HgX molekule. Kemijsko vezanje u AuX uspoređeno je s vezanjem u HgX uzevši u obzir efekte relativnosti, prijenosa naboja i ionskog vezivanja, troelektronsko vezivanje u usporedbi s dvoelektronskim vezivanjem, rezidualno π-vezivanje, odbijanje slobodnih elektronskih parova, te efekt d-elektrona. Međuigra različitih elektronskih efekata vodi do bitno različitih trendova izračunatih energija disocijacije veze, koji se mogu objasniti jednostavnim MO modelom temeljenim na razlikama u elektronegativnosti, atomskim orbitalnim energijama i njihovoj promjeni uslijed skalarne relativnosti. Relativistički utjecaj na energije disocijacije veze direktno je povezan s relativističkim promjenama u energiji 6s orbitala i elektronskoj gustoći.